bond-making step itself based on the size of the ligand.

Previous studies showed[26,23] that large distal side steric effects in proteins and in heme cyclophanes do not appreciably change dissociation rates k_1 for either CO or RNC. We now find that bond formation k_{-1} is also unaffected. These conclusions differ only slightly, but significantly, from the interpretation of steric effects based upon crystal structures and low-temperature kinetic studies.[10] The steric effect in adamantane heme is related to the steric effect in converting the protein-separated geminate pair to the contact pair. This process requires moving the adamantane moiety in the model and moving the distal imidazole (or other blocking group) in myoglobin. Although we suggest that the largest steric effect in heme proteins is on entry into the protein (assembly of the protein-separated pair [Hm ‖ L] from distinct-solvated species), we find evidence for further steric effects in the process which converts the protein-separated pair to the contact pair [Hm L]. This interpretation is consistent with the general four-state model of heme protein ligation proposed by Frauenfelder et al.[10] as well as the trajectory calculations of Karplus and Case.[42]

Previous studies demonstrated that the steric effects on binding dioxygen and carbon monoxide to adamantane heme cyclophane and other cyclophanes are essentially identical as judged by changes in association rates.[27,29] Recent studies of the kinetics of dioxygen and carbon monoxide binding to mutants of myoglobin in which the distal blocking group was changed[43] also demonstrate the same effects for each mutation, within a factor of about two, on rates of binding the two diatomic ligands. These similarities in model and myoglobin behavior add further evidence that there is a "local steric effect" operating near the iron in myoglobin. This steric effect could differentiate ligands on the basis of their size or shape, since they must fit into the contact pair space, but not on the basis of the angle of the Fe–X–Y bound state, because the steric effect operates before the bonding step. We, therefore, conclude that distal steric effects are identical for the diatomic ligands CO, NO, and O_2 in all the steps leading to ligation. The current results, taken together with previous studies, therefore, provide strong evidence that CO and O_2 are differentiated in their binding to model compounds and to heme proteins by polar effects (or hydrogen bonding effects) on dioxygen dissociation rates.

(42) Case, D. A.; Karplus, M. *J. Mol. Biol.* **1979**, *132*, 343.
(43) Springer, B. A.; Egeberg, K. D.; Sligar, S. G.; Rohlfs, R. J.; Mathews, A. J.; Olson, J. S. *J. Biol. Chem.* **1989**, *264*, 3057.

Conclusion

Subpicosecond laser flash photolysis of two very different types of sterically hindered heme model compounds and measurement of geminate recombination from the resulting heme ligand contact pairs allow us to draw the following conclusions about steric effects on the geminate recombination process and on overall ligand binding: trans strain, which distorts heme planarity, reduces geminate recombination by an amount comparable to changes in overall combination rates, whereas blocking (frontal) steric effects, which do not alter heme planarity, have little effect on geminate return. Since blocking does exert tremendous influence on the overall combination rate, we conclude that blocking affects the assembly of the contact pair rather than bond making. Ligands of different size are not distinguished much in the geminate return (bond-forming) process; size discrimination occurs in the assembly of the contact pair. These conclusions should apply broadly to all metalloporphyrins and heme complexes; we conjecture that they will apply to some other metal complexes, particularly those that have limited fluxional mobility, and may be pertinent to free-radical geminate processes as well.

Acknowledgment. This research was supported in part by the National Institutes of Health Grants HL-13581 and RR02353-01 and the National Science Foundation Grant CHE-8715561. We thank Dr. N. Koga for his chemical syntheses.

Mechanism of Ligand Binding to Hemes and Hemoproteins. A High-Pressure Study

Douglas J. Taube,[†] Hans-Dieter Projahn,[‡] Rudi van Eldik,*[,‡] Douglas Magde,*[,†] and Teddy G. Traylor*[,†]

Contribution from the Department of Chemistry, D-006, University of California, San Diego, La Jolla, California 92093, and Institute for Inorganic Chemistry, University of Witten/Herdecke, Stockumer Strasse 10, 5810 Witten, FRG. *Received December 29, 1989*

Abstract: The effect of pressure on the recombination kinetics of small ligands binding to sperm whale myoglobin, protoheme dimethyl ester, and monochelated protoheme was studied with use of laser flash photolysis. The volumes of activation observed indicate that in both the protein and the models bond formation is the rate-determining step only for carbon monoxide, while for oxygen, isocyanides, and 1-methylimidazole almost no bond formation occurs in the transition state of the observed reaction. The effect of pressure on the escape of carbon monoxide, oxygen, and methyl isocyanide from the heme pocket of sperm whale myoglobin was also investigated. The volume increase observed for all ligands during this process is attributed to a "gatelike" conformational change in the protein. The results are discussed in terms of the previously proposed three- and four-state reaction schemes for model hemes and myoglobin, respectively.

Introduction

The mechanistic understanding of the binding of small neutral molecules to ferrous hemes and hemoproteins has attracted significant attention in recent years.[1-7] Model complexes are usually employed to improve our understanding of the reactions of the corresponding proteins. The application of picosecond and nanosecond laser flash photolysis techniques[8] has suggested that in

* Authors to whom correspondence should be addressed.
† University of California, San Diego.
‡ University of Witten/Herdecke.

(1) Armstrong, G. D.; Sykes, A. G. *Inorg. Chem.* **1986**, *25*, 3135.
(2) Paul, J.; v. Goldammer, E.; Wenzel, H. R. *Z. Naturforsch., C: Biosci.* **1988**, *43*, 162.
(3) Ansari, A.; Berendzen, J.; Braunstein, D.; Cowen,. B. R.; Frauenfelder, H.; Hong, M. K.; Iben, I. E. T.; Johnson, J. B.; Ormos, P.; Sauke, T. B.; Scholl, R.; Schulte, A.; Steinbach, P. J.; Vittitow, J.; Young, R. D. *Biophys. Chem.* **1987**, *26*, 337.

0002-7863/90/1512-6880$02.50/0

simple model compounds the germinate pair [Fe L] exists as a single kinetic intermediate:

$$Fe\text{-}L \rightleftharpoons [Fe\ L] \rightleftharpoons Fe + L \qquad (1)$$

In proteins, on the other hand, the germinate pair exists in two very different configurations: a fast-reacting "contact pair" and a slow-reacting "separated pair".[9] In the separated pair, the ligand wanders through the heme pocket before re-forming the contact pair that is the immediate precursor to bond formation.

The application of high-pressure techniques in mechanistic studies of inorganic and organometallic systems has contributed significantly toward a better understanding of ligation processes.[10-12] Such techniques have also been applied with success in the study of bioinorganic and biochemical systems.[13,14] The determination of volumes of activation and the associated construction of reaction volume profiles have become essential for the unequivocal assignment of mechanisms. We have therefore undertaken a detailed investigation of the effect of pressure up to 200 MPa on the binding kinetics of small neutral molecules to ferrous hemes and hemoproteins. Contributions from bond formation/breakage, solvation/desolvation, spin changes, and geometrical changes are expected to determine the overall pressure effect. The selected hemes do not decompose or denature under pressure up to 400 MPa.[4,13-20] The results of this study add a further dimension to recent studies of the effect of pressure on the formation and deoxygenation kinetics of oxymyoglobin.[21,22]

Experimental Section

Materials. Model Compounds. Protoheme dimethyl ester chloride ($PHDME^+Cl^-$) was dissolved in a minimum volume of CH_2Cl_2, and the solution was then added to 4 mL of toluene so that the absorbance of the Soret band was 0.5 in a 1-cm cell, $[PHDME^+Cl^-] \approx 1 \times 10^{-6}$ M. For the $(RNC)_2$ complexes (R = Me, *t*-Bu), 5×10^{-3}–1×10^{-2} M RNC was syringed into the toluene. The sample and about 200 mg of zinc amalgam were placed into a tonometer. The solution was deoxygenated by several freeze–pump–thaw (f–p–t) cycles and placed under Ar. The sample was stirred overnight to ensure complete reduction to the $PHDME(RNC)_2$ complex. The $(1MeIm)_2$ complex was prepared in a similar fashion ($[1MeIm] = 1 \times 10^{-2}$ M), except that after the f–p–t cycles the sample was placed under CO.

The monochelated protoheme (MCPH) samples were prepared by adding a minimum volume of CH_2Cl_2 to $MCPH^+Cl^-$ and then adding this solution to 4 mL of toluene so that the absorbance of the Soret band was 0.5 in a 1-cm cell. The solution was then transferred to a tonometer with a total volume of 140.4 mL and bubbled with CO for 1 h. The solution was reduced by the addition of a few microliters of a saturated solution of sodium dithionite/18-crown-6 in methanol. For the O_2 sample, a minimum amount of reducing agent was used. The O_2 sample was degassed by several f–p–t cycles and placed in the tonometer under Ar, and 1 mL of CO and 7 mL of O_2 were added by syringe.

Following the preparation of the samples in the tonometer, the samples were anaerobically cannulated into a pill box cell for further studies.[23,24]

The sperm whale myoglobin samples were prepared following published procedures.[9]

Instrumentation. The photolysis setup consists of a Lumonics 861T XeCl excimer laser that is used to pump a Lumonics EPD-330 dye laser. The gain medium is coumarin 540 in methanol. The output pulses at 540 nm have a duration of 4 ns and an energy of 3 mL at a repetition rate of 1 Hz and are used as a photolysis source. The photolysis beam intersects the observation beam at right angles in the sample cell. The observation lamp is either a xenon flash lamp for reaction rates $>10^5$ s^{-1} or a continuous-wave tungsten lamp for reaction rates $<10^4$ s^{-1}. A small Bausch & Lomb monochromator restricts the probe light to a 5-nm bandwidth before the sample. A lens focuses the beam into the center of the pill box cell. After the sample, the probe light is passed through a blue Corning glass filter, focused into the slit of a J-Y H20 monochromator, and detected by an Amperex 56 TUVP photomultiplier. The signal is sent to a Biomation waveform recorder, Model 6500 (for the fast reactions, 1024 data points per laser shot) or 805 (for the slow reactions, 2048 data points per laser shot), interfaced to a microcomputer. Several digitized traces (up to 1023) were averaged for an improved signal to noise ratio. The data are transferred to a Celerity 1260D minicomputer for analysis or are directly evaluated on the microcomputer.

A compact, transportable high-pressure unit complete with a four-window high-pressure cell was used in this investigation.[25] The cell is equipped with a thermostating coil (±0.1 °C) and is pressurized with water up to 200 MPa. A mechanical hydraulic (oil) pump and a separator unit are used for this purpose.[25] A pill box sample cell[23] with a 1.4-cm path length at ambient pressure was placed inside the pressure cell. This sample cell has several advantages that make it ideal for the study of photochemical processes.[11]

Results and Discussion

Model Heme Complex Studies. The ability to photolyze six-coordinate ferrous heme complexes to produce five-coordinate heme species has been known since the last century and studied quantitatively for the past three decades.[26] In our experiments, an axial ligand was photodissociated from a six-coordinate ferrous heme and the bimolecular recombination to form the original complex was monitored (eq 2). The reaction was studied in the

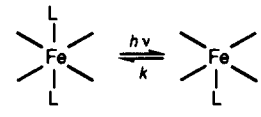

(2)

region of maximum absorbance difference between the five- and six-coordinate species, i.e., the Soret region (400–450 nm). The kinetics were run under pseudo-first-order conditions ([L] ≫ [heme]) in a sealed pill box cell at 25 °C. The only variable was the applied pressure (up to 200 MPa). The volume of activation was determined from the slope ($=-\Delta V^{\ddagger}/RT$) of a plot of ln *k* versus pressure.[10,12] We preferred to study the $PHDME(RNC)_2$ system instead of the (1MeIm)PHDME(RNC) system for RNC = MeNC and *t*-BuNC, since the quantum yield for the formation of the fully solvated ligand is ≈1.0 in the former complex, compared to only 0.33 in the latter case.[8] When CO is the ligand photodissociated, formation of the fully solvated ligand also occurs with near 100% efficiency.

The volumes of activation for the bimolecular addition of O_2 and 1MeIm were determined by the Gibson technique.[27] The Gibson technique was used because (1) the O_2 complex is unstable, ultimately oxidizing the iron to the ferric state, and (2) the quantum yield for the formation of the free five-coordinate complex from the $(1MeIm)_2$ complex is only 0.04.[28] The Gibson

(4) Coletta, M.; Ascenzi, P.; Traylor, T. G.; Brunori, M. *J. Biol. Chem.* **1985**, *260*, 4151.
(5) Perutz, M. F.; Fermi, G.; Luisi, B.; Shaanan, B.; Liddington, R. C. *Acc. Chem. Res.* **1987**, *20*, 309.
(6) Shikama, K. *Coord. Chem. Rev.* **1988**, *83*, 73.
(7) Frauenfelder, H.; Wolynes, P. G. *Science (Washington, D.C.)* **1985**, *229*, 337.
(8) Traylor, T. G.; Magde, D.; Taube, D.; Jongeward, K. *J. Am. Chem. Soc.* **1987**, *109*, 5864.
(9) Jongeward, K. A.; Magde, D.; Taube, D. J.; Marsters, J. C.; Traylor, T. G.; Sharma, V. S. *J. Am. Chem. Soc.* **1988**, *110*, 380.
(10) van Eldik, R.; Ed. *Inorganic High Pressure Chemistry: Kinetics and Mechanisms*; Elsevier: Amsterdam, 1986.
(11) Kotowski, M.; van Eldik, R. *Coord. Chem. Rev.* **1989**, *93*, 19.
(12) van Eldik, R.; Asano, T.; le Noble, W. J. *Chem. Rev.* **1989**, *89*, 549.
(13) Heremans, K. In ref 10, Chapter 7.
(14) Weber, G. In *High Pressure Chemistry and Biochemistry*; van Eldik, R., Jonas, J., Eds.; NATO ASI C197. Reidel: Dordrecht, 1987; p 401.
(15) Gibson, Q. H.; Carey, F. G. *J. Biol. Chem.* **1977**, *252*, 4098.
(16) Ogunmola, G. B.; Zipp, A.; Chen, F.; Kauzmann, W. *Proc. Natl. Acad. Sci. U.S.A.* **1977**, *74*, 1.
(17) Fisher, M. T.; Scarlata, S. F.; Sligar, S. G. *Arch. Biochem. Biophys.* **1985**, *240*, 456.
(18) Gibson, Q. H.; Carey, F. G. *Biochem. Biophys. Res. Commun.* **1975**, *67*, 747.
(19) Morishima, I.; Ogawa, S.; Yamada, H. *Biochemistry* **1980**, *19*, 1569.
(20) Alden, R. G.; Satterlee, J. D.; Mintorovitch, J.; Constantinidis, I.; Ondrias, M. R. *J. Biol. Chem.* **1989**, *264*, 1933.
(21) Projahn, H.-D.; Dreher, C.; van Eldik, R. *J. Am. Chem. Soc.* **1990**, *112*, 17.
(22) Adachi, S.; Morishima, I. *J. Biol. Chem.* **1989**, *264*, 18896.
(23) le Noble, W. J.; Schlott, R. *Rev. Sci. Instrum.* **1976**, *47*, 770.
(24) Wieland, S.; van Eldik, R. *Rev. Sci. Instrum.* **1989**, *60*, 955.
(25) Spitzer, M.; Gartig, F.; van Eldik, R. *Rev. Sci. Instrum.* **1988**, *59*, 2092.
(26) Ainsworth, S.; Gibson, Q. H. *Nature (London)* **1957**, *180*, 1416.
(27) Traylor, T. G.; Tsuchiya, S.; Campbell, D.; Mitchell, M.; Stynes, D.; Koga, N. J. *J. Am. Chem. Soc.* **1985**, *107*, 604.

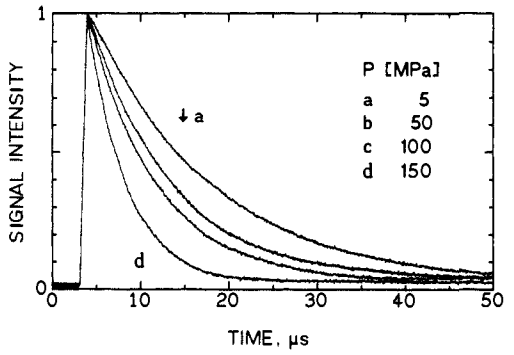

Figure 1. Trace of signal intensity versus time as a function of pressure for the reaction MCPH–CO ⇌ MCPH + CO. Conditions: solvent, toluene; λ_{obs} = 440 nm; T = 25 °C; [MCPH] = 15 μM; [CO] = 6.7 mM.

Table I. Volumes of Activation for the Bimolecular Addition of Various Ligands to Five-Coordinate Fe(II) Model Heme Complexes[a]

heme complex	ligand	$\Delta V^{\ddagger}$, cm^3 mol^{-1}	k_{on},[c] M^{-1} s^{-1}
MCPH	CO	−19.3 ± 0.4	(1.08 ± 0.02) × 10^7
MCPh[b]	O_2	−11.3 ± 1.0	(1.04 ± 0.04) × 10^8 9.0 × 10^7[d]
(MeNC)PHDME	MeNC	11.6 ± 0.8	(3.93 ± 0.04) × 10^8 2.8 × 10^8[d]
(*t*-BuNC)PHDME	*t*-BuNC	9.9 ± 1.0	(2.46 ± 0.01) × 10^8
(1MeIm)PHDME[b]	1MeIm	10.9 ± 3.1	(1.48 ± 0.04) × 10^8

[a] Experimental conditions: solvent, toluene; T = 25 °C; P = 5–150 MPa; [MCPh] = 15 μM; [PHDME] = 15 μM; [MeNC] = 3.4 mM; [*t*-BuNC] = 1.1 mM; [1MeIm] = 10.5 mM; [CO] = 6.7 mM (based on L(CO, toluene) = 8.9 μM Torr^{-1},[41,42] P(CO) = 760 Torr); [O_2] = 0.3 mM (based on L(O_2, toluene) = 7.3 μM Torr^{-1},[41,42] P(O_2) = 40 Torr). [b] Gibson technique: [1MeIm]/[CO] = 11; [O_2]/[CO] = 6. [c] Mean value of at least six kinetic runs, each run average of 400 laser shots; rate constants for P = 5 MPa. [d] Reference 27.

technique involves the formation of a thermodynamic product, the heme–CO complex, and a kinetic product, the heme–O_2 or the heme–1MeIm complex. The photolysis of the heme–CO complex generates the five-coordinate heme intermediate with near 100% quantum efficiency. The ratio $k^{L}[L]/k^{CO}[CO]$ is sufficiently high so that more than 95% of the kinetic product formed is the heme–L species (L = O_2 or 1MeIm) (eq 3).

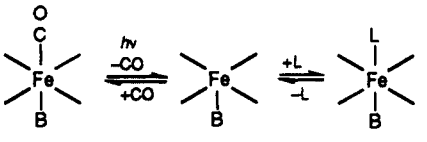

(3)

For the systems investigated here, the trans ligand B does not undergo photodissociation. The thermal dissociation rates for both the heme–O_2 and the heme–1MeIm are large enough so that the equilibrium heme–CO complex is re-formed within 1 s. Therefore, the direct observation of the bimolecular addition of O_2 (Figure 1) and 1MeIm to the five-coordinate heme was accomplished. A summary of the observed results is given in Table I, which also lists the conditions used. Figure 2 shows the plot of ln k versus pressure for all five of the ligands investigated.

We have previously described a three-state mechanism for the binding of ligands to model heme systems[8] (eq 4). In eq 4, Hm–L

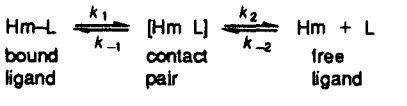

(4)

is the bound, six-coordinate heme and Hm + L is the five-coordinate heme and the fully solvated ligand. The intermediate [Hm L] is a "contact pair" in which the ligand has moved far enough away from the iron to form the five-coordinate heme but the ligand and iron are in the same solvent cage. The lifetime

(28) Momenteau, M.; Lavalette, D. *J. Am. Chem. Soc.* **1978**, *100*, 4322.

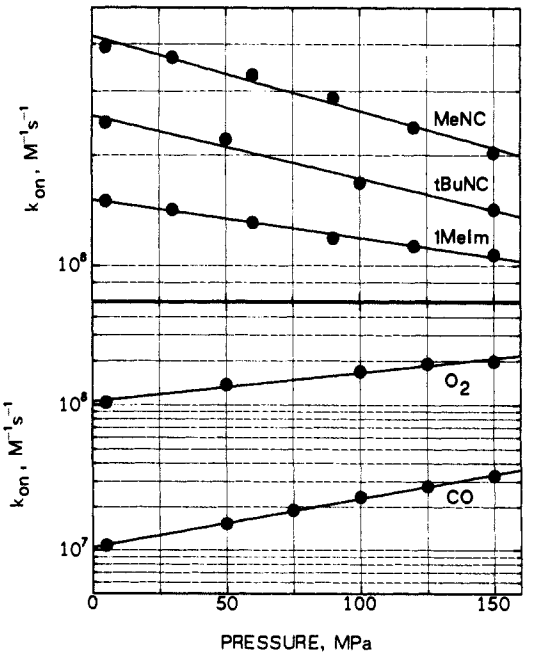

Figure 2. Logarithmic plot of k_{on} versus pressure for the reaction Hm + L → Hm–L (L = MeNC, *t*-BuNC, 1MeIm, CO, O_2). Conditions: see Table I.

of the contact pair is on the order of 10–30 ps for low-viscosity fluids. The bimolecular association rate, k_{on}, can be expressed in terms of the proposed mechanism in eq 4 by (5), if we assume

$$k_{on} = k_{-2}k_{-1}/(k_{-1} + k_2) = k_{-2}\Phi \qquad (5)$$

that k_1 is negligible. In this model, bimolecular association involves two distinct steps: (1) diffusion through the bulk solvent and partial desolvation to form the contact pair, described by k_{-2}, and (2) bond formation from the contact pair, which occurs with efficiency Φ. During its lifetime in the contact pair, the ligand can either form a bond or diffuse away again into the solvent. In previous studies,[8] the contact pair was created by subpicosecond flash photolysis. In this report, we examine whether the same model is useful in understanding bimolecular recombination studied as a function of pressure, for which the contact pair must be formed by normal thermal processes.

Table I shows that the values of $\Delta V^{\ddagger}$ range from −19 to +12 cm^3 mol^{-1} for the association of various ligands with model heme complexes. There is a clear correlation between $\Delta V^{\ddagger}$ and k_{on}. This is explained in terms of a change in the rate-limiting step of mechanism 4, which implies different limits for eq 5 and, therefore, different factors dominating $\Delta V^{\ddagger}$.

As we have shown,[8] ligands such as isocyanaides and 1MeIm re-form the iron–ligand bond efficiently from the contact pair following subpicosecond photolysis ($\Phi_{ambient}$ > 60%). On the other hand, CO rebinds poorly from the contact pair with $\Phi_{ambient}$ < 5%. In unpublished work, we have increased the viscosity of the CO system and observed that the rate constant for bond-making k_{-1} is some 50–100 times slower than for isocyanides and 1MeIm. It is of interest that the ligands that show significant rebinding from the photolytically generated contact pair, which include RNC, 1MeIm, and O_2, all have bimolecular association rate constants of about 2 × 10^8 M^{-1} s^{-1}, whereas CO, which binds only very slightly from the contact pair, has a much smaller bimolecular association rate constant of 1 × 10^7 M^{-1} s^{-1}. In other words, CO is the only ligand for which recombination is reaction limited; all other ligands are close to the diffusion limit.

It is helpful to note that by using ln k_{on} = ln k_{-2} + ln Φ from (5) and the definition of $\Delta V^{\ddagger}$, we may express $\Delta V^{\ddagger}$ as the sum of two terms

$$\Delta V^{\ddagger} = \Delta V^{\ddagger}(k_{-2}) + \Delta V^{\ddagger}(\Phi) \qquad (6)$$

where $\Delta V^{\ddagger}(k_{-2})$ describes the effect of pressure on the formation

of the contact pair and $\Delta V^{\ddagger}(\Phi)$ the effect of pressure on the probability of bond formation within the contact pair.

Consider the effect of pressure along a reaction coordinate for an entering ligand.

First, the reaction partners must diffuse together. The pressure dependence of the viscosity of toluene is large,[29] with $\Delta V^{\ddagger}_{v} = +22$ cm^3 mol^{-1}. Diffusion coefficients are expected[29] to display $\Delta V^{\ddagger}$ that are close to $\Delta V^{\ddagger}_{v}$. Consequently, there is a large positive contribution to $\Delta V^{\ddagger}(k_{-2})$ that is similar for all ligands. The next step involves partial desolvation of both iron and ligand in the process of forming the contact pair in the same solvent cage. This is expected also to make a positive contribution to $\Delta V^{\ddagger}(k_{2})$, but one that varies somewhat with ligand. Together, these effects ensure that $\Delta V^{\ddagger}(k_{-2})$ is positive and large for toluene as the solvent.

Once that contact pair has formed, its fate is determined by competition between two processes. Escape from the cage k_2 should have a positive $\Delta V^{\ddagger}$ and be slower at higher pressures. However, the effect of k_2 is exerted on the denominator of Φ, so it makes a negative contribution to $\Delta V^{\ddagger}(\Phi)$. Bond formation k_{-1}, which is accompanied by a high-spin to low-spin transition of the ferrous center, should have a negative volume of activation[10,12] that directly contributes a negative $\Delta V^{\ddagger}$. Consequently, both effects make negative contributions to $\Delta V^{\ddagger}(\Phi)$.

There is, however, a limit to how large Φ can become, namely $\Phi_{max} = 1$, and this sets a limit to how negative $\Delta V^{\ddagger}(\Phi)$ can become. If we assume that $\Delta V^{\ddagger}(\Phi)$ is approximately constant over the range investigated, $0.1 < P < 200$ MPa, so that

$$\Delta V^{\ddagger}(\Phi) = -RT\Delta(\ln \Phi)/\Delta P \quad (7)$$

we can take $\Delta P = 200$ MPa and choose as a conservative upper limit

$$\Delta(\ln \Phi) = \ln \Phi_{ambient} - \ln 1 = \ln \Phi_{ambient} \quad (8)$$

To cite a numerical example, if $\Phi_{ambient} = 0.66$, then $\Delta V^{\ddagger}(\Phi)$ cannot be more negative than about -5 cm^3 mol^{-1}. Since Φ is already large at ambient pressure, it cannot increase very much. This is the situation in the diffusion-controlled limit, where the overall bimolecular process should be dominated by $\Delta V^{\ddagger}(k_{-2})$. It we assume that the limiting value of Φ is reached earlier, say at 100 MPa, despite the fact that the plots do not show curvature at that pressure, $\Delta V^{\ddagger}(\Phi)$ could be as large as -10 cm^3 mol^{-1}.

Of the ligands investigated, the two isocyanides and 1MeIm all have large, positive $\Delta V^{\ddagger}$. They also react at the diffusion-controlled limit of 2×10^8 M^{-1} s^{-1}. The increased reaction rate compared to the gaseous ligands may be due to the large dipole moment of the isocyano group, which facilitates interaction with the positively charged iron atom.[30] The rate-determining step is characterized by k_{-2}, and the transition state controlling the overall reaction occurs as the ligand enters the contact pair. On the other hand, even these ligands do not lie in the extreme diffusion limit. Presumably, Φ becomes larger as pressure is increased and contributes a modest negative contribution to the overall $\Delta V^{\ddagger}$.

In contrast, carbon monoxide "visits" the contact pair about 20 times before it binds. The rate-determining step for CO association is the bond-making process. The positive contributions of $\Delta V^{\ddagger}(k_{-2})$ are outweighed by the large, negative contribution for $\Delta V^{\ddagger}(\Phi)$ due to the collapse of the contact pair, accompanied by spin changes, and the reduced escape from the cage.

The volume of activation for the bimolecular association of O_2 to MCPH lies between those for RNC and CO. This appears to be a borderline case. The positive contributions to $\Delta V^{\ddagger}$ due to increasing viscosity and partial desolvation fail to overrule the large negative contributions arising from bond formation and reduced cage escape. Even so, the observed negative value can only be explained if $\Phi_{ambient}$ is smaller than for RNC and k_{-2} correspondingly larger. There are a number of differences between

(29) Isaacs, N. S.; *Liquid Phase High Pressure Chemistry*; Wiley: New York, 1981; p 106.

(30) Olson, J. S.; McKinnie, R. E.; Mims, M. P.; White, D. K. *J. Am. Chem. Soc.* **1983**, *105*, 1522.

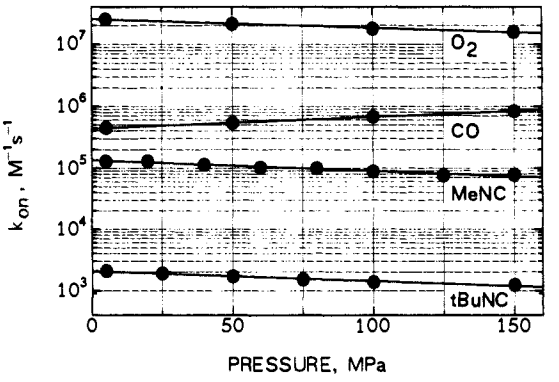

Figure 3. Logarithmic plot of k_{on} versus pressure for the reaction Mb + L → Mb-L (L = MeNC, *t*-BuNC, CO, O_2). Conditions: see Table II.

Table II. Volumes of Activation for the Bimolecular Addition of Various Ligands to Deoxy Sperm Whale Myoglobin in Aqueous Buffer[a]

ligand	$\Delta V^{\ddagger}$, cm^3 mol^{-1}	k_{on},[b] M^{-1} s^{-1}
CO	-10.0 ± 0.8	$(5.2 \pm 1.8) \times 10^5$
O_2	5.2 ± 0.5	$(2.5 \pm 0.2) \times 10^7$[c]
O_2	7.8 ± 1.3	$(1.3 \pm 0.3) \times 10^7$[d]
MeNC	8.8 ± 1.0	$(1.4 \pm 0.1) \times 10^5$
		1.2×10^5[e]
t-BuNC	9.3 ± 0.3	$(2.1 \pm 0.1) \times 10^3$

[a] Experimental conditions: solvent, water; 0.05 M bis-Tris buffer; ionic strength, 0.1 M (NaCl); pH = 7.0; $T = 25$ °C; $P = 5$–150 MPa; [Mb] = 20 μM; [CO] = 0.98 mM; [MeNC] = 4–20 mM; [*t*-BuNC] = 4.4–29.5 mM. [b] Mean value of at least three kinetic runs, each run average of 400 laser shots; rate constants for $P = 5$ MPa. [c] Reference 21. [d] Reference 33. [e] Reference 27.

O_2 and the other ligands that are expected to influence how k_{-1} and k_2 are affected by pressure. The spin state of O_2 is a triplet, in contrast to the other ligands, all of which are singlets. Only O_2 is "double-ended" as a reactant. Finally, O_2 is small and nonpolar.

All the $\Delta V^{\ddagger}$ are slightly less positive or more negative than might be expected. Perhaps the volume of activation for diffusion of small ligands is not quite as large as the volume of activation for kinetmatic viscosity or perhaps the contribution from desolvation is actually negative by a small amount, contrary to expectations.

Sperm Whale Myoglobin Studies

Bimolecular Association. The effect of pressure on the bimolecular association rate was examined for sperm whale myoglbin reacting with CO, O_2, MeNC, and *t*-BuNC in water as the solvent. Figure 3 shows the variation with pressure of the bimolecular rate constants, which are defined by the overall mechanism of eq 9.

$$\text{Mb-L} \underset{k_{on}}{\overset{h\nu}{\rightleftharpoons}} \text{Mb} + \text{L} \quad (9)$$

Volumes of activation calculated from the slopes of those plots are displayed in Table II along with available literature data, most notably the data for O_2 as the ligand.

We have shown previously[9] that reactions of ligands with Mb require at least a four-state mechanism: In eq 10, Mb-L is the

$$\underset{\text{bound ligand}}{\text{Mb-L}} \underset{k_{-1}}{\overset{k_1}{\rightleftharpoons}} \underset{\text{contact pair}}{[\text{Mb L}]} \underset{k_{-2}}{\overset{k_2}{\rightleftharpoons}} \underset{\text{protein-separated pair}}{[\text{Mb}||\text{L}]} \underset{k_{-3}}{\overset{k_3}{\rightleftharpoons}} \underset{\text{free ligand}}{\text{Mb} + \text{L}} \quad (10)$$

liganded myoglobin complex with six-coordinated iron and Mb + L is deoxymyoglobin along with the slovated ligand diffusing separately through the solvent. The first intermediate [Mb L] is a contact pair in which the ligand is displaced sufficiently to yield the spectrum of deoxymyoglobin with five-coordinated iron but remains in close proximity to the iron and, consequently, can re-form the bond. The protein-separated pair [Mb||L] is an

intermediate in which the ligand has rotated or translated slightly and the amino acids near the binding site have rearranged slightly so that bond re-formation is not possible until the favorable contact pair is regenerated, but the ligand remains in the protein "pocket" and has not exchanged with ligands free in solution. The lifetime of the contact pair is in the range of tens of picoseconds, while the protein separated pair has a lifetime 3 orders of magnitude longer, some tens of nanoseconds.[9]

The relation of the overall bimolecular rate constant k_{on} to the elementary steps of mechanism 10 is complex. Even with the justified simplifications that k_1 is negligible and that $k_{-1}, k_2 \gg k_{-2}, k_3$, one has

$$k_{on} = \frac{k_{-3}k_{-2}k_{-1}/(k_{-1} + k_2)}{k_{-2}k_{-1}/(k_{-1} + k_2) + k_3} = \frac{k_{-3}k'}{k' + k_3} = k_{-3}\Phi \quad (11)$$

Note that Φ is a probability for bond formaiton once the ligand is in the protein. It is useful to write the overall $\Delta V^{\ddagger}$ as the sum of two terms

$$\Delta V^{\ddagger} = \Delta V^{\ddagger}(k_{-3}) + \Delta V^{\ddagger}(\Phi) \quad (12)$$

where $\Delta V^{\ddagger}(k_{-3})$ characterizes the effect of pressure on diffusion through the solvent and initial desolvation in the process of entering the protein, and $\Delta V^{\ddagger}(\Phi)$ characterizes the effect of pressure on all processes that take place in the protein and together affect the probability that the encounter pair will ultimately form an iron–ligand bond. As before, one expects $\Delta V^{\ddagger}(k_{-3}) > 0$ and $\Delta V^{\ddagger}(\Phi) < 0$. However, there are some important differences in detail between the protein systems and the models.

In strong contrast to toluene, the viscosity of water exhibits almost no pressure dependence near room temperture,[29] with $\Delta V^{\ddagger}_{\eta} = +0.16$ cm^3 mol^{-1}. Any large, positive contribution must involve desolvation and entry of the ligand into the protein.

Bond-making is expected to have a substantial negative $\Delta V^{\ddagger}$; however, it may be reduced somewhat by the surrounding protein, which is generally less compressible than water and serves a biological function in insulating the active site from environmental influences (of which pressure might be important for sperm whales?). Serveral studies[15-20] have pointed out that volume changes associated with iron high-to-low spin transitions are about -10 cm^3 mol^{-1}. This value is much greater than that associated with the geometrical changes that occur during the spin state conversion of the iron porphyrin and must be attributed to volume changes of the entire protein[20]. In this respect, it is interesting to note that some workers[31,32] have reported values of about -10 cm^3 mol^{-1} for the high-to-low spin transition of other iron(II) model compounds with polydentate nitrogen-donor ligands. It is difficult to predict the effect of pressure on k_2 and k_{-2}. One might expect comparable effects of opposite sign that tend to offset each other in their effect on Φ. One expects k_3 to have a substantial positive volume of activation, which affects the denominator of Φ and, consequently, makes a negative contribution to $\Delta V^{\ddagger}(\Phi)$. Direct experimental data in support of that expectation are described below. We conclude that $\Delta V^{\ddagger}(\Phi)$ is surely negative, even if it is difficult to untangle the various processes involved in the four-state model. However, Φ is bounded so that $\Delta V^{\ddagger}(\Phi)$, while negative, will be small in the case of any ligand for which Φ is already large at ambient pressure.

The $\Delta V^{\ddagger}$ for the bimolecular association rate constants in Table II for MeNC and *t*-BuNC are +8.8 and +9.3 cm^3 mol^{-1}, respectively. For CO, we measure -10.0 cm^3 mol^{-1}, compared to -9.2 cm^3 mol^{-1} in a recent report.[22] The value for O_2 lies in between at +5.2 cm^3 mol^{-1}, as measured previously by some of us,[21] +4.6 cm^3 mol^{-1} in another study,[22] or +7.8 cm^3 mol^{-1} according to a third.[33] The agreement in the few measurements that have been repeated is good, especially considering the variation

Table III. Partial Molar Volumes for the Ligands Studied

ligand	density, g cm^{-3}	fw	V^m, cm^3 mol^{-1}
t-BuNC	0.735	83	113
1MeIM	1.03	82	80
MeNC	0.73	41	56
CO	0.79[a]	28	35
O_2	1.14[a]	32	28

[a] At boiling point.

measured for horse and dog myoglobin instead of sperm whale.[22] A similarity with the model compounds is apparent. Most notable is the fact that again CO stands out as the unique ligand, characterized by a substantial negative $\Delta V^{\ddagger}$. Consequently, it is likely that the transition state for its overall combination is very "productlike", and the rate-limiting step is bond formation with accompanying spin changes. Since a high-to-low spin transition is facilitated by an increase in pressure,[19] it is understandable that the association reaction of CO speeds up with pressure. However, escape from the protein, k_3, is also an important parameter that makes a negative contribution of $\Delta V^{\ddagger}(\Phi)$.

All the remaining ligands show positive $\Delta V^{\ddagger}$ for the overall reaction, despite a wide range of values for k_{on}. It was demonstrated previously[9] that the variation in k_{on} among O_2, MeNC, and *t*-BuNC must be due to variation in k_3, for they all have very large Φ, 0.83,[34] 0.76,[9] and 0.53,[9] respectively. For comparison, the value for CO is only 0.04.[35] The reciprocals of these, 1.15, 1.3, 1.9, and 25, translate into the number of times that a ligand enters the protein before it binds to iron. The transition state that dominates the overall ligation occurs when the ligand enters the protein (k_{-3}), except for CO. Since it was argued above on a priori grounds that one expects $\Delta V^{\ddagger}(k_{-3})$ to be positive and $\Delta V^{\ddagger}(\Phi)$ to be negative, one expects all ligands except CO to have positive overall $\Delta V^{\ddagger}$.

The fact that k_{-3} varies strongly with the size of the ligand and that it has a substantial pressure dependence, which cannot be due simply to a viscosity change in water, since there is very little change, suggests that it is quite appropriate to imagine that there is a "gate" governing the entry of ligands into the protein, as proposed a decade ago.[36,37] The contributions to $\Delta V^{\ddagger}(k_{-3})$ include a modest effect of pressure on mobility, for reasons more subtle than just kinematic viscosity, any protein distortion required to admit the ligand, and the important effect of desolvation. There are differences among the ligands that influence all of these. The isocyanides are a little larger than the diatomic molecules. In addition, they have a definite dipole (negative and toward the terminal carbon) while CO and O_2 are effectively apolar. This is shown by the large dipole moment of MeNC (3.85 D), compared to CO (0.11 D) and O_2 (0.0 D).[38] This should cause the isocyanides to be more strongly solvated in the polar aqueous solvent than the nonpolar CO and O_2 and to have a decreased mobility as the pressure is increased. As the ligand enters the protein, it must desolvate to a great extent to get through the protein gate. For the isocyanides, this will result in an increase in $\Delta V^{\ddagger}$ due to the tight solvent structure around these ligands. In addition, small conformational changes may also occur in the protein under pressure, and the gate of the protein pocket may constrict under pressure. The gate opening will be more important in the case of the larger isonitriles RNC than for CO and O_2 (see Tables III), resulting in a larger volume effect for these ligands.

Nanosecond Geminate Recombination. Although most of the parameters of both the three-state and the four-state models can only be measured with picosecond measurements, k_3, which

(31) DiBenedetto, J.; Arkle, V.; Goodwin, H. A.; Ford, P. C. *Inorg. Chem.* **1985**, *24*, 455.
(32) McGarvey, J. J.; Lawthers, I.; Heremans, K.; Toftlund, H. *J. Chem. Soc., Chem. Commun.* **1984**, 1575.
(33) Hasinoff, B. B. *Biochemistry* **1974**, *13*, 3111.
(34) Gibson, Q. H.; Olson, J. S.; McKinnie, R. E.; Rohlfs, R. J. *J. Biol. Chem.* **1986**, *261*, 10228.
(35) Henry, E. R.; Sommer, J. H.; Hofrichter, J.; Eaton, W. A. *J. Mol. Biol.* **1983**, *166*, 443.
(36) Case, D. A.; Karplus, M. *J. Mol. Biol.* **1979**, *132*, 343.
(37) Beece, D.; Eisenstein, L.; Frauenfelder, H.; Good, D.; Marden, M. C.; Reinisch, L.; Reynolds, A. H.; Sorensen, L. B.; Yue, K. T. *Biochemistry* **1980**, *19*, 5147.
(38) Dipole moments in the gas phase: *CRC Handbook of Chemistry and Physics*, 62nd ed.; CRC Press: Boca Raton, FL, 1982; E-60.

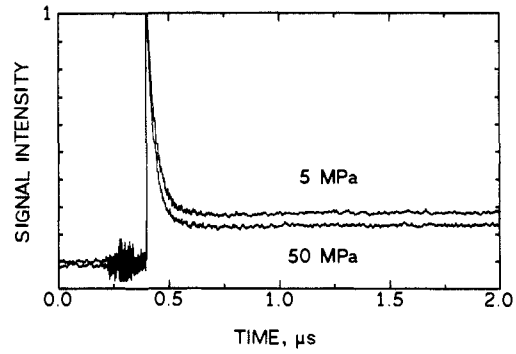

Figure 4. Trace of signal intensity versus time as a function of pressure for the reaction Mb||MeNC ⇌ Mb + MeN. Conditions: λ_{obs} = 440 nm; T = 25 °C; ionic strength, 0.1 M (NaCl); 0.05 M bis-Tris buffer; [Mb] = 15 μM; [MeNC] = 6 mM.

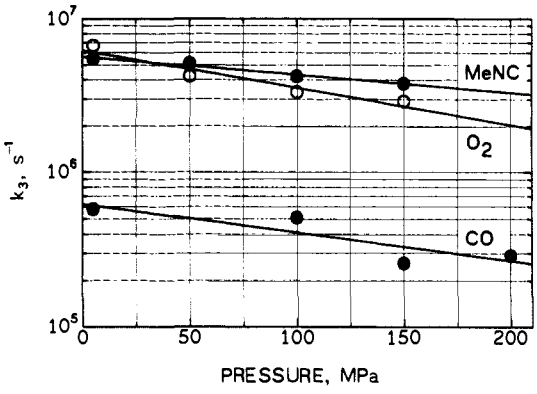

Figure 5. Logarithmic plot of k_3 versus pressure for the reaction Mb||L → Mb + L (L = MeNC, CO, O_2). Conditions: see Table IV.

characterizes ligand escape from the protein to the surrounding solvent, is accessible from nanosecond experiments by way of eq 13. Here, k_{gem} is the observed rate constant for the nanosecond

$$k_3 = k_{gem}\Gamma_C \tag{13}$$

process and Γ_C is the amount of escape from the protein-separated pair. Γ_C may be calculated from eq 14, where A is the amplitude

$$\Gamma_C = B/(A + B) \tag{14}$$

of the first-order process and B the zero offset of the geminate reaction, i.e., $\Delta A(t = \infty)/\Delta A(t = 0)$.[8] Here, $t = \infty$ is a time of several hundred nanoseconds at which recombination from all geminate pairs is complete but bimolecular recombination has not commenced, and $t = 0$ is understood on the nanosecond (not picosecond) time scale.

Figure 4 shows the increase of the five-coordinate deoxymyoglobin at 438 nm immediately following photolysis of the myoglobin–MeNC complex. The decrease in the absorbance is attributed to the concentration-independent re-formation of the Fe–MeNC bond from the protein-separated pair. The end point of the first-order process does not reach the prephotolysis baseline. The remaining deoxymyoglobin is a result of the MeNC ligand escaping the protin and diffusing into the solvent. As the pressure is increased, the most obvious change in Figure 4 is the slight decrease in the end point of the geminate reaction. This means that less of the MeNC escapes from the protein into the solvent; therefore, k_3 decreases with increasing pressure. This is shown in Figure 5, where ln k_3 is plotted versus pressure for the three ligands investigated (L = MeNC, CO, and O_2).

A more dramatic effect of pressure upon the escape of a ligand from the protein is seen with carbon monoxide. Figure 6 shows the effect of pressure upon the geminate return of CO to sperm whale myoglobin. At ambient pressure (or at 5 MPa), we have not been able to observe geminate return of CO to myoglobin.[9] As the pressure was increased to 100, 150, and 200 MPa, the amount of return from the protein-separated pair increases from

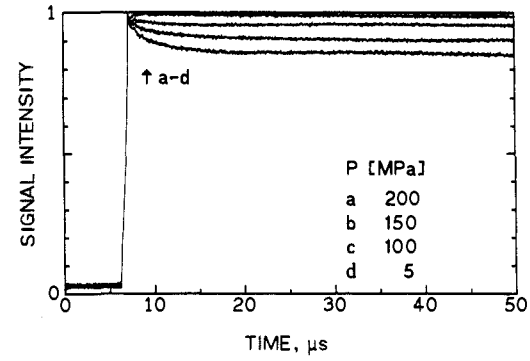

Figure 6. Trace of signal intensity versus time as a function of pressure for the reaction Mb||CO ⇌ Mb + CO. Conditions: λ_{obs} = 440 nm; T = 25 °C; ionic strength, 0.1 M (NaCl); 0.05 M bis-Tris buffer; pH = 7.0; [Mb] = 15 μM; [CO] = 0.98 mM.

Table IV. Volumes of Activation for the Escape of the Ligand from the Protein-Separated Pair, to the Solvated Ligand (k_3), for Various Ligands[a]

ligand	$\Delta V^{\ddagger}$, $cm^3\ mol^{-1}$	k_3,[b] s^{-1}
CO	11.7 ± 1.1	(5.8 ± 0.9) × 10^5
O_2[c]	12.6 ± 1.7	(5.9 ± 1.1) × 10^6
MeNC	9.1 ± 3.5	(5.5 ± 0.1) × 10^6

[a] Experimental conditions: solvent, water; 0.05 M bis-Tris buffer; ionic strength, 0.1 M (NaCl); T = 25 °C; pH = 7.0; P = 5–200 MPa; [Mb] = 15 μM; [CO] = 0.98 mM; [O_2] = 1.3 mM; [MeNC] = 6 mM. [b] Mean value of at least three kinetic runs, each run average of 1024 laser shots; rate constants for P = 5 MPa. [c] pH = 8.5.

2.4 and 6.3 to 12.1%, respectively. This translates into a volume of activation of +11.7 $cm^3\ mol^{-1}$. The values of k_3 and the $\Delta V^{\ddagger}$ for k_3 are collected in Table IV. One other $\Delta V^{\ddagger}(k_3)$ value was reported recently[22] for O_2 and sperm whale myoglobin. Our number is 25% smaller.

All the values of $\Delta V^{\ddagger}(k_3)$ are large and positive, consistent with the notion of a "gate" that operates in both directions. They, therefore, contribute to a negative value for $\Delta V^{\ddagger}(\Phi)$, as expected. We expect the pressure dependence of k_3 to reflect both small conformational changes in the protein and the solvation of the exiting ligand. The fact that the isocyanides differ from the diatomic molecules much less upon exiting than upon entering is explained if the protein pocket is already slightly distorted when it contains an isocyanide, which is larger and more polar than CO or O_2. The protein exploits steric effects to discriminate among ligands at entry to the protein; no major discrimination is possible between the two small diatomic molecules. The latter differ primarily in bond forming and bond breaking, affected by the protein in different ways. A recent study[39] involving site-directed mutations confirmed that His E7 is a very important protein residue. In addition to restricting the size of the sixth coordination position, the distal histidine is also capable of discriminating between O_2 and CO by stabilizing oxygen with a hydrogen bond.[40]

Since the data reported here include only nanosecond measurements and not picosecond studies, it would be reasonable to treat them with a simpler three-state model, as used in dozens of other studies of hemoprotein photolyses at ambient temperature. One could even assign an "effective overall" volume of activation for the complex of processes involved in forming the contact pair and making a bond. We prefer not to do that and hope that we will soon be able to report measurements on the picosecond kinetics.

(39) Springer, B. A.; Egeberg, K. D.; Sligar, S. G.; Rohlfs, R. J.; Mathews, A. J.; Olson, J. S. *J. Biol. Chem.* **1989**, *264*, 3057.
(40) Mims, M. P.; Porras, A. G.; Olson, J. S.; Noble, R. W.; Peterson, J. A. *J. Biol. Chem.* **1983**, *258*, 14219.
(41) Messer Griesheim GmbH. *Gase Handbuch*; Messer Briesheim: Frankfurt, 1986.
(42) D'Ans-Lax. *Taschenbuch für Chemiker und Physiker. Band I. Makroskopische physikalisch-chemische Eigenschaften*; Springer Verlag: Berlin, Heidelberg, 1967.

Conclusions

In a previous report,[8] we proposed that the binding of ligands to ferrous porphyrins should be described by a three-state mechanism. Here, we report the studies of the bimolecular association rates under applied solution pressure. The positive volumes of activation for the bimolecular association of MeNC, *t*-BuNC, and 1MeIm to five-coordinate model heme complexes indicate that the rate-controlling transition state occurs as the ligand enters the "contact pair". The large negative volume of activation for the bimolecular association of CO to MCPH indicates that the transition state for binding occurs in the bond-making process. The smaller negative value for O_2 suggests an intermediate case.

The bimolecular association of ligands to sperm whale myoglobin, as well as the escape of the ligands from the protein, has been studied under pressure. Isocyanide ligands and O_2 have a positive volume of activation in which the overall transition state for ligation is attributed to the ligand entering the protein. The transition state for the bimolecular association of CO to deoxymyoglobin is assigned to the bond-making process on account of its negative volume of activation.

The volumes of activation for the escape of ligands from the protein to the solvent are all positive. This can be attributed to a conformational change of the protein that is required as the ligand leaves the heme pocket.

These pressure studies are well understood within the three- and four-state models previously proposed. They add support for the basic concept and behavior of the intermediates postulated.

Acknowledgment. This research was supported in part by National Institutes of Health Grants HL13581 (T.G.T.) and RR02353-01 and National Science Foundation Grant CHE-8715561 (D.M.). Support from the Duetsche Forschungsgemeinschaft and the Fonds der Chemischen Industrie is gratefully acknowledged (R.v.E.).

Registry No. (MeNC)PHDME, 128218-29-1; (*t*-BuNC)PHDME, 128218-30-4; CO, 630-08-0; O_2, 7782-44-7; MeNC, 593-75-9; *t*-BuNC, 7188-38-7.

Hydrogen Atom Transfer Reactions of Transition-Metal Hydrides. Kinetics and Mechanism of the Hydrogenation of α-Cyclopropylstyrene by Metal Carbonyl Hydrides

R. Morris Bullock* and Edward G. Samsel

Contribution from the Department of Chemistry, Brookhaven National Laboratory, Upton, New York 11973. *Received January 8, 1990*

Abstract: The hydrogenation of α-cyclopropylstyrene (CPS) by a series of metal carbonyl hydrides (MH) gives a mixture of the unrearranged hydrogenation product $Ph(CH_3)(c\text{-}C_3H_5)CH$ (UN) and the rearranged hydrogenation product (*E*)-$Ph(CH_3)C{=}CHCH_2CH_3$ (RE). With the exception of $HCr(CO)_3Cp$, second-order kinetics are found, conforming to the rate law $-d[CPS]/dt = k[CPS][MH]$. The proposed mechanism involves hydrogenation by sequential hydrogen atom transfers from the metal hydride to the organic substrate. The rate-determining step is the first hydrogen atom transfer in which a carbon-centered radical and a metal-centered radical are formed. In the case of $HCr(CO)_3Cp$ at 22 °C, the equilibrium constant for this step is $K \sim 10^{-12}$. The effect of the significant amount of 17-electron $^{\bullet}Cr(CO)_3Cp$ radical formed in the hydrogenation of CPS by $HCr(CO)_3Cp$ is accommodated by the kinetic analysis. Since the initially formed carbon-centered radical undergoes first-order ring-opening rearrangement in competition with second-order trapping by MH, analysis of the product ratio as a function of [MH] concentration provides relative rates of hydrogen atom transfer from metal hydrides to a carbon-centered radical. Relative rates of hydrogen atom transfer at 60 °C from MH to **1** are as follows: $k_{rel} = 1$ for $HMn(CO)_4PPh_3$, $k_{rel} = 4$ for $HMo(CO)_3(C_5Me_5)$, $k_{rel} = 93$ for $HMo(CO)_3Cp$, $k_{rel} = 94$ for $HFe(CO)_2(C_5Me_5)$. Comparison of the hydrogenation of CPS by $HW(CO)_3Cp$ and $DW(CO)_3Cp$ indicates that the kinetic isotope effect is inverse ($k_{HW}/k_{DW} = 0.55$) for the first hydrogen atom transfer but normal ($k_{HW}/k_{DW} = 1.8$-2.2) for the second hydrogen atom transfer. The first hydrogen atom transfer is endothermic, and its rate is largely influenced by the strength of the M-H bond. Steric effects appear to exert a dominant influence on the rate of the second hydrogen atom transfer, which is exothermic. Kinetic and mechanistic experiments indicate that hydrogenation of 2-cyclopropylpropene by $HCr(CO)_3Cp$ also occurs by a radical pathway.

Organometallic reactions involving odd-electron pathways and free-radical intermediates have become increasingly well-recognized.[1] A prominent example is the homolytic cleavage of the M-H bond of a metal hydride, resulting in hydrogen atom transfer reactions. A seminal study by Sweany and Halpern[2] provided definitive evidence that the hydrogenation of α-methylstyrene by $HMn(CO)_5$ proceeds by a free-radical mechanism. Several lines of evidence, including the observation of an inverse kinetic isotope effect ($k_H/k_D \approx 0.4$) and CIDNP effects in the NMR, were consistent with a mechanism involving sequential hydrogen atom transfers from the metal hydride to the organic substrate. Similar hydrogen atom transfer reactions have been proposed to occur in the hydrogenation of substituted styrenes,[3] anthracenes,[4] all-

(1) For reviews treating various aspects of free radical mechanisms, metal radicals, and hydrogen atom transfer, see: (a) Halpern, J. *Pure Appl. Chem.* **1986**, *58*, 575-584; **1979**, *51*, 2171-2182. (b) Brown, T. L. *Ann. N.Y. Acad. Sci.* **1980**, *333*, 80-89. (c) Tyler, D. R. *Prog. Inorg. Chem.* **1988**, *36*, 125-194. (d) Trogler, W. C. *Int. J. Chem. Kinet.* **1987**, *19*, 1025-1047. (e) Baird, M. C. *Chem. Rev.* **1988**, *88*, 1217-1227. (f) Eisenberg, D. C.; Norton, J. R. *Isr. J. Chem.*, in press.

(2) Sweany, R. L.; Halpern, J. *J. Am. Chem. Soc.* **1977**, *99*, 8335-8337.

(3) (a) Sweany, R. L.; Comberrel, D. S.; Dombourian, M. F.; Peters, N. A. *J. Organomet. Chem.* **1981**, *216*, 57-63. (b) Roth, J. A.; Orchin, M. *J. Organomet. Chem.* **1979**, *182*, 299-311. (c) Nalesnik, T. E.; Orchin, M. *J. Organomet. Chem.* **1980**, *199*, 265-269. (d) Nalesnik, T. E.; Freudenberger, J. H.; Orchin, M. *J. Organomet. Chem.* **1981**, *221*, 193-197; *J. Mol. Catal.* **1982**, *16*, 43-49; *J. Organomet. Chem.* **1981**, *236*, 95-100. (e) Nalesnik, T. E.; Orchin, M. *Organometallics* **1982**, *1*, 222-223. (f) Matsui, Y.; Orchin, M. *J. Organomet. Chem.* **1983**, *244*, 369-373. (g) Ungváry, F.; Markó, L. *Organometallics* **1982**, *1*, 1120-1125; *J. Organomet. Chem.* **1983**, *249*, 411-414. (h) Nalesnik, T. E.; Orchin, M. *J. Organomet. Chem.* **1981**, *222*, C5-C8. (i) Bockman, T. M.; Garst, J. F.; King, R. B.; Markó, L.; Ungváry, F. *J. Organomet. Chem.* **1985**, *279*, 165-169. (j) Roth, J. A.; Wiseman, P. *J. Organomet. Chem.* **1981**, *217*, 231-234. (k) Roth, J. A.; Wiseman, P.; Ruszala, L. *J. Organomet. Chem.* **1983**, *240*, 271-275.

0002-7863/90/1512-6886$02.50/0